PHYSICAL REVIEW B VOLUME 2, NUMBER 6 15 SEPTEMBER 1970

Electric-Field-Induced Infrared Absorption and Raman Scattering in Diamond*

E. Anastassakis†‡ and E. Burstein
Physics Department and Laboratory for Research of the Structure of Matter, University of Pennsylvania, Philadelphia, Pennsylvania 19104
(Received 30 March 1970)

We present a detailed discussion of our experimental results on the effect of an externally applied static electric field on the absorption of EM radiation by the $\vec{q}\approx 0$ optical modes of diamond. It is shown that the normally infrared-inactive long-wavelength vibrational modes can become infrared active in the presence of the field. From the strength of the field-induced infrared absorption, we determine the absolute value for the Raman tensor of these modes, and its dependence on the field through a higher-order effect. The latter effect also manifests itself as a change in the intensity and/or the polarization selection rules of the first-order Raman scattering.

I. INTRODUCTION

Crystals of diamond structure have three optica vibrational branches which are degenerate at the center of the Brillouin zone. The symmetry character of the $\vec{q}\approx 0$ optical vibrational modes is described by the three-dimensional irreducible representation (IRR) F_{2g} of the crystal point group (O_h). In first order these modes are Raman (R) active and infrared (IR) inactive. (These crystals exhibit well-defined, although weak, absorption bands, owing to higher-order terms in the crystal electric moment.[1])

From a phenomenological point of view, first-order IR absorption and first-order R scattering arise from terms in the electric moment (per unit cell) $\vec{M}$, and symmetric electronic polarizability (per unit cell) $\overleftrightarrow{\alpha}$, respectively, which are linear in the relative displacement of the atoms, i.e.,

$$\vec{M}_j=\left(\frac{\partial \vec{M}}{\partial u_j}\right)\cdot \vec{u}_j=\overleftrightarrow{e}_j\cdot \vec{u}_j\,, \tag{1a}$$

$$\overleftrightarrow{\alpha}_j=\left(\frac{\partial \overleftrightarrow{\alpha}}{\partial u_j}\right)\cdot \vec{u}_j=\overleftrightarrow{a}_j\cdot \vec{u}_j\,, \tag{1b}$$

where $\vec{u}_j$ is the atomic-displacement normal coordinate of the lattice-vibrational mode (j), and exhibits the symmetry of the mode (j). $\overleftrightarrow{e}_j$ and $\overleftrightarrow{a}_j$ are the effective-charge and the R tensor per unit cell, respectively, associated with the mode (j).

The strength of the first-order IR absorption and R scattering is proportional to $|\overleftrightarrow{e}_j|^2$ and $|\overleftrightarrow{a}_j|^2$, respectively. Whether or not the parameters $\overleftrightarrow{e}_j$ and $\overleftrightarrow{a}_j$ are nonzero for a particular crystal and mode symmetry is determined by the symmetry of the mode. Such properties have been designated as "mode properties."[2] For the symmetry of the three $\vec{q}\approx 0$ degenerate optical modes of diamond-type crystals one finds from simple symmetry arguments that $\overleftrightarrow{e}_{F_{2g}}=0$ and $\overleftrightarrow{a}_{F_{2g}}\neq 0$. Accordingly, the F_{2g} optical modes of these crystals are IR inactive and R active in first order.

The experimental determination of $\overleftrightarrow{a}_j$ through a measurement of the absolute intensity of R scattering is not feasible in general. A very rough theoretical estimate of $\overleftrightarrow{a}_j$ for homopolar semiconductors has only been obtained by Loudon,[3] based on deformation potential arguments. The purpose of the present work is to demonstrate the possibility of determining $\overleftrightarrow{a}_j$ experimentally by carrying out IR absorption measurements. The method used is based on the fact that new effects may be possible in a crystal if the symmetry of the crystal is lowered by the application of an external force. Such effects have been designated as "morphic effects."[4] A general discussion and symmetry analysis of the morphic effects in connection with lattice dynamical processes is given elsewhere.[2]

We are presently concerned with the morphic effect of inducing first-order IR absorption by an IR-inactive mode, by applying a static electric field. It was first shown by Burstein and Ganesan,[5] and by Szigeti[6] that an externally applied static electric field may induce an effective ionic charge on the atoms of diamond-type crystals which is linear with the field. Under these conditions, one would expect the $\vec{q}\approx 0$, IR inactive, and triply degenerate mode, to become IR active and nondegenerate in general. Experimentally this would be observed as an absorption band at the frequency of the mode (1332 cm^{-1} for diamond). An electric-field-induced IR absorption by crystal vibrational modes was first observed in diamond.[7] It is, in essence, the same effect as that predicted by Con-

don[8] for homonuclear molecules, and observed experimentally by Crawford and Dagg[9,10] for H_2 molecules.

The induced effective charge associated with an applied electric field at the frequency ω_a is given in the case of diamond-type crystals, by[11]

$$e_{F_{2g}E} = \frac{\partial\alpha(\omega_a)}{\partial u_{F_{2g}}} \quad E_a \quad , \tag{2}$$

where $\alpha(\omega_a)$ is the electronic polarizability at the frequency ω_a. Since for diamond there is no optical phonon contribution to the polarizability, α and $\partial\alpha/\partial u_{F_{2g}}$ are essentially independent of ω (provided ω is well below the absorption edge for interband transitions) and one can then set $\partial\alpha(\omega_a)/\partial u_{F_{2g}}$ equal to $\overleftrightarrow{a}_{F_{2g}}$, the R tensor at optical frequencies. The strength of the field-induced absorption band is proportional to the square of the field-induced electric moment. The latter is proportional to the field-induced effective charge $\overleftrightarrow{e}_{F_{2g}E}$ given by Eq. (2). Thus, from the measured strength of the field-induced absorption one can determine the field-induced effective charge, and thereby deduce an absolute value for the R tensor $\overleftrightarrow{a}_{F_{2g}}$. Any deviation from a quadratic dependence of the observed strength of the induced IR absorption on the applied field will simply indicate that $\overleftrightarrow{a}_{F_{2g}}$ itself exhibits a dependence on the applied field.

The relation between $\overleftrightarrow{a}_{F_{2g}}$ and phenomenological and experimental parameters is established in Secs. II and III, while our detailed experimental results are presented in Sec. IV. The dependence of $\overleftrightarrow{a}_{F_{2g}}$ on the applied field is then examined in Sec. V in connection with IR absorption. This leads naturally to the effect that an applied field may be expected to have on the R activity of the R-active mode F_{2g}. The symmetry aspects of this and our experimental results are presented in Sec. VI.

II. FIELD-INDUCED ABSORPTION CONSTANT

The contribution of the field-induced absorption of the EM radiation by the $\vec{q}\approx 0$ optical phonons to the frequency-dependent dielectric constant is given by[12,13]

$$\epsilon^E_{\mu\nu}(\omega) = \frac{4\pi N}{\overline{m}} \sum_j \frac{m^E_\mu(j,0)m^E_\nu(j,0)}{\omega(j,0,E)^2 - \omega^2 - i\omega\gamma(j,0,E)} \ , \tag{3a}$$

where

$$m^E_\mu(j,0) = e_{\mu\sigma}(j)\,\hat{d}_\sigma(j), \tag{3b}$$

$$e_{\mu\sigma}(j) = a_{\mu\lambda,\sigma}(j)E_\lambda \quad . \tag{3c}$$

Summation rules are implied over any repeated index. $\overline{m}$ is the reduced mass of the atoms in the unit cell, N is the number of unit cells per unit volume, $\hat{d}_\sigma(j)$ is the σ component of the polarization vector of the jth $\vec{q}\approx 0$ optical phonon, $e_{\mu\sigma}(j)$ and $a_{\mu\lambda,\sigma}(j)$ are the $\mu\sigma$ and $\mu\lambda\sigma$ components of the field-induced effective charge $\overleftrightarrow{e}_{jE}$ and atomic R tensor $\overleftrightarrow{a}_j$, respectively, for the same optical phonon, and $\omega(j,0,E)$ and $\gamma(j,0,E)$ are the frequency and damping constant of this phonon, in the presence of a static field $\vec{E}$.[14–16] For the diamond structure, which has a center of symmetry, the change of $\omega(F_{2g},0,E)$ and $\gamma(F_{2g},0,E)$ will be even in the electric field.[17] They are treated here as empirical parameters. A (6×3) matrix notation can be used for the R tensor of diamond. The row index runs from 1 to 6 and stands for a suppressed index[18] of the two indices $(\mu\lambda)$ designating the polarizations $\hat{\epsilon}_0$ and $\hat{\epsilon}_a$ of the incident and applied field, respectively. The column index (1, 2, 3) stands for the phonon polarization $\hat{d}(j)$. In this matrix notation, the R tensor, when referred to the system of the crystallographic axes $\hat{x}=[100]$, $\hat{y}=[010]$, $\hat{z}=[001]$, takes the form

$$\overleftrightarrow{a}_{F_{2g}} = a \begin{bmatrix} 0 & 0 & 0 \\ 0 & 0 & 0 \\ 0 & 0 & 0 \\ 1 & 0 & 0 \\ 0 & 1 & 0 \\ 0 & 0 & 1 \end{bmatrix} \quad , \tag{4a}$$

where a is the single independent component of the R tensor for the F_{2g} mode. This form is equivalent to the three (3×3) matrices appearing in the review tables of Ref. 19 for the F_{2g} mode of the O_h structure, i. e.,

$$\overleftrightarrow{a}_{F_{2g}} \begin{pmatrix} 0 & 0 & 0 \\ 0 & 0 & a \\ 0 & a & 0 \end{pmatrix}, \begin{pmatrix} 0 & 0 & a \\ 0 & 0 & 0 \\ a & 0 & 0 \end{pmatrix}, \begin{pmatrix} 0 & a & 0 \\ a & 0 & 0 \\ 0 & 0 & 0 \end{pmatrix},$$

$$u_{F_{2g}}: \quad (yz) \quad , \quad (zx) \quad , \quad (xy) \quad , \tag{4b}$$

where (yz), (zx), (xy) are the three basis functions of the F_{2g} irreducible representation, according to which $u_{F_{2g}}$ transforms [the matrices (4b) are referred to the xyz system]. In three-index notation, $a_{F_{2g}}$ can also be written as $a|e_{\mu\lambda\sigma}|$, where $e_{\mu\lambda\sigma}$ is the Levi-Civita function.

At this point, it is more convenient to consider the specific configurations used in the present experiment. The schematic diagram is shown in Fig. 1. In Table I. the orientation of the sample axes $x'y'z'$ relative to the crystallographic axes xyz is given, together with the dimensions of the two type-IIa diamond samples $C1$ and $C2$ which were used. As it is easier to work out the quantitative analysis using the set of $x'y'z'$ axes, which coin-

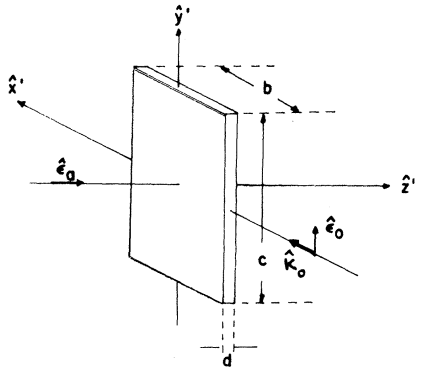

FIG. 1. Schematic presentation of the diamond plates used in these experiments. The light wave vector $\vec{k}_0$ (and therefore $\vec{q}_0$) is along $\hat{x}'$ and the applied electric field along $\hat{z}'$.

cide with the laboratory axes, rather than the axes xyz, we will refer all vector and tensor properties to the system $x'y'z'$. The rotated form of $\overleftrightarrow{a}_{F_{2g}}$ in (6×3) matrix notation is given below as $\overleftrightarrow{a}(C1)$ and $\overleftrightarrow{a}(C2)$ for the two configurations $C1$ and $C2$, respectively,

$$\overleftrightarrow{a}(C1)=a\begin{bmatrix}0&0&-1\\0&0&1\\0&0&0\\0&1&0\\-1&0&0\\0&0&0\end{bmatrix}\quad\begin{matrix}\hat{x}'\parallel[1\bar{1}0]\\,\ \hat{y}'\parallel[110]\,,\\\hat{z}'\parallel[001]\end{matrix}\qquad(5a)$$

$$\overleftrightarrow{a}(C2)=-\frac{a}{\sqrt{3}}\begin{bmatrix}\sqrt{2}&0&1\\-\sqrt{2}&0&1\\0&0&-2\\0&1&0\\1&0&0\\0&-\sqrt{2}&0\end{bmatrix}\quad\begin{matrix}x'\parallel[11\bar{2}]\\,\ y'\parallel[\bar{1}10]\\z'\parallel[111]\end{matrix}\ .\qquad(5b)$$

From now on, all vector and tensor indices 1, 2, 3 are referred to the $x'y'z'$ system of axes, respectively, unless otherwise indicated.

The polarization selection rules for the field-induced IR absorption can be written in full tensor notation as follows[7]:

$$\hat{\epsilon}_{0\mu}\,a_{\mu\lambda,\sigma}(j)\,\hat{d}_\sigma(j)\,\hat{\epsilon}_{a\lambda}\neq0\,,\qquad(6)$$

where summation rules are implied. With $\hat{\epsilon}_a\parallel\hat{z}'$ and $\vec{k}_0\parallel\hat{x}'$, the incident EM radiation $\hat{\epsilon}_0$ can be polarized either along or at right angle to the applied field. Thus using $\overleftrightarrow{a}(C1)$, $\overleftrightarrow{a}(C2)$, and Eq. (6), one can find which components of $\hat{\epsilon}_a$, $\hat{d}(j)$ and $\hat{\epsilon}_0$ satisfy Eq. (6). The results for $C1$ and $C2$ and for the two possible polarizations of $\hat{\epsilon}_0$ are summarized in Table II. TO_1 and TO_2 stand for the TO modes polarized along y' and z', respectively.

TABLE I. Orientation and dimensions of the two type-IIa diamond samples which were used in these experiments.

Sample	$\hat{x}'$	$\hat{y}'$	$\hat{z}'$	b (mm)	c (mm)	d (mm)	l^a (mm)
$C1$	$[1\bar{1}0]$	$[110]$	$[001]$	3.4	8.0	0.74	2.4
$C2$	$[11\bar{2}]$	$[\bar{1}10]$	$[111]$	2.3	9.6	1.0	1.6

[a] l is the effective light path.

It should be noticed that the polarization selection rules described by Eq. (6) become the same as those for the first-order R scattering if one replaces the applied field $\hat{\epsilon}_a$ by the scattered field $\hat{\epsilon}_s$. An obvious consequence of this is that for the induced IR absorption one may expect transverse as well as longitudinal optical modes to be involved. For cubic crystals, the intrinsic IR absorption involves only transverse optical modes.

We now proceed to establish the relation between the field-induced effective charge $\overleftrightarrow{e}_{F_{2g}}$ and the field-induced absorption constant at the mode frequency ω_j. If we consider the $C1$ geometry, we find from $\overleftrightarrow{a}(C1)$ and Eq. (3) that the only nonzero components of the field-induced dielectric constant at frequency ω are $\epsilon_{22}^E(\omega)$ and $\epsilon_{11}^E(\omega)$, where

$$\epsilon_{22}^E(\omega)=\frac{4\pi N}{\overline{m}}\,\frac{m_2^E(\mathrm{TO}_1)m_2^E(\mathrm{TO}_1)}{\omega(\mathrm{TO}_1)^2-\omega^2-i\omega\gamma(\mathrm{TO}_1)}\,,\qquad(7a)$$

$$m_2^E(\mathrm{TO}_1)=e_{22}(\mathrm{TO}_1)\,d_2(\mathrm{TO}_1)\,,\qquad(7b)$$

$$e_{22}(\mathrm{TO}_1)=a_{23,2}E_3=aE\ .\qquad(7c)$$

TABLE II. The results of the polarization selection rules for the field-induced IR absorption.[a]

Sample	$\hat{\epsilon}_0$	$a_{\mu\lambda,\sigma}$	$\hat{d}(j)$	Type of phonon
$C1$	$\hat{y}'$	$a_{23,2}=a$	$\hat{y}'$	TO_1
$C1$	$\hat{z}'$	$a_{33,3}=0$	...	...
$C2$	$\hat{y}'$	$a_{23,2}=-\frac{a}{\sqrt{3}}$	$\hat{y}'$	TO_1
$C2$	$\hat{z}'$	$a_{33,3}=\frac{2a}{\sqrt{3}}$	$\hat{z}'$	TO_2

[a] The field is applied along $\hat{z}'$ and the incident EM radiation $\hat{\epsilon}_0$ is sent along $\hat{x}'$. The indices 1, 2, 3 are referred to the $x'y'z'$ axes, respectively. The matrices $\overleftrightarrow{a}(C1)$ and $\overleftrightarrow{a}(C2)$ and Eq. (6) have been used. The single independent component of the R tensor for diamond is designated by a.

An identical expression holds for $\epsilon_{11}^{E}(\omega)$ involving a LO-type phonon and the component $a_{13,1}=a$. The total dielectric constant is given by

$$\overleftrightarrow{\epsilon}(\omega)\simeq\epsilon_0\overleftrightarrow{I}+\overleftrightarrow{\epsilon}^{E}(\omega)=\begin{bmatrix}\epsilon_0+\epsilon_{11}^{E}(\omega) & 0 & 0\\ 0 & \epsilon_0+\epsilon_{22}^{E}(\omega) & 0\\ 0 & 0 & \epsilon_0\end{bmatrix}, \quad (8)$$

where ϵ_0 is the static dielectric constant, and $\overleftrightarrow{I}$ is a (3×3) unit matrix. With $\vec{k}\parallel\hat{x}'$ and $\vec{k}\cdot\vec{\mathcal{E}}=0$, where $\vec{\mathcal{E}}=\hat{\epsilon}_0\mathcal{E}(\omega)$, it turns out from the EM wave equation which has the form

$$\vec{k}\times(\vec{k}\times\vec{\mathcal{E}})+\left(\frac{\omega}{c}\right)^2\overleftrightarrow{\epsilon}(\omega)\cdot\vec{\mathcal{E}}=0\,, \quad (9)$$

that there are two solutions for k^2, given by

$$k^2=(\omega/c)^2\,(\epsilon_0+\epsilon_{22}^{E}) \quad \text{for } \hat{\epsilon}_0\parallel\hat{y}'\perp\hat{\epsilon}_a\,, \quad (10a)$$

$$k^2=(\omega/c)^2\epsilon_0 \quad \text{for } \hat{\epsilon}_0\parallel\hat{z}'\parallel\hat{\epsilon}_a\,. \quad (10b)$$

This indicates that for the $C1$ configuration only the component of the EM radiation along y' is absorbed, whereas the component along z' is transmitted through the crystal as if there were no field applied. (This result is consistent with the one obtained from the polarization selection rules, i.e., Table II.) We therefore need to consider only the relation (10a) in deriving an expression for the peak absorption constant, $\Delta A(\omega)$ at $\omega=\omega(\mathrm{TO}_1)$. $\Delta A(\omega)$ is related to the imaginary part of the wave vector $k=k_1+ik_2$ by

$$\Delta A=2k_2\,. \quad (11)$$

From Eqs. (7), (10), and (11) one finds that

$$\Delta A=\Omega^2/\gamma(\mathrm{TO}_1)\eta_1 c\,, \quad (12)$$

where η_1 is the real part of the refraction index in the presence of a field, and

$$\Omega=(4\pi N e_{22}^2/\overline{m})^{1/2} \quad (13)$$

is an effective plasma frequency. η_1 can be set to a very good approximation equal to $\epsilon_0^{1/2}$. By repeating the analysis for the $C2$ orientation, we find that

$$\Delta A=\Omega^2/3\gamma(\mathrm{TO}_1)\eta_1 c \quad \text{for } \hat{\epsilon}_0\parallel\hat{y}'\perp\hat{\epsilon}_a$$
$$=4\Omega^2/3\gamma(\mathrm{TO}_2)\eta_1 c \quad \text{for } \hat{\epsilon}_0\parallel\hat{z}'\parallel\hat{\epsilon}_a\,. \quad (14)$$

Equations (12) and (14) give the field-induced absorption constant at $\omega(j)$. Fortunately the absorption due to two-phonon processes in the vicinity of ω_j is negligible for diamond ($A<0.2$ cm^{-1} in type IIa). It is for this reason that diamond is a unique material for this experiment (it also has a fairly high dielectric-breakdown voltage). Attempts to observe the effect in Si were unsuccessful; first, because the background absorption of the lattice due to two-phonon processes in the vicinity of ω_j, the frequency of the $\vec{q}\approx0$ optical phonon, was high enough to mask the field effect ($\simeq2$ cm^{-1} for Si) and second, because it was not possible to apply sufficiently high fields without excessive heating of the crystal. (A rough estimate of the R tensor for these materials can be obtained indirectly from the ratio of their first-order R intensities to that of diamond.[20,21])

III. EXPERIMENTAL

A. Techniques

For a typical transmission experiment, we designate the incident and transmitted light intensity, the transmittance of the sample, and the recorder reading by I_0, I, $T=I/I_0$, and S, respectively. Since the quantities I, T, and S are proportional to each other, their relative changes are equal, i.e., $\Delta I/I=\Delta T/T=\Delta S/S$. In the course of an experiment, it is the ratio $\Delta S/S$ which can be determined directly from the recorder readings. Thus the ratio $\Delta T/T$ can be immediately determined. To establish a relation between the observed ratio $\Delta T/T$ and the change ΔA of the crystal absorption constant A, we use the well-known equation of transmission for normal incidence and multireflections, i.e.,

$$T=(1-R)^2e^{-Al}/(1-R^2e^{-2Al})\,, \quad (15)$$

where R is the reflectivity, A the absorption constant, and l is an effective light path defined as the length of that crystal region where the absorption occurs. In the present experiment, the absorption region is determined as the crystal region under the applied field. The estimated values for l are given in Table I. The reflectivity is given by

$$R=[(\eta-1)^2+\kappa^2]/[(\eta+1)^2+\kappa^2]\,, \quad (16)$$

where η is the refractive index, and κ the extinction coefficient. In the infrared, κ is negligible for diamond. The numerical values for η and the other physical constants which we use are given in Table III. Using these, we find from Eqs. (15) and (16), in very good approximation, that

$$\Delta T/T=-1.06l\Delta A\,. \quad (17)$$

We note that no specific assumption has been made about the origin of the changes ΔI or ΔT.

The first observation of the field-induced IR absorption in diamond was based on a comparison of the recordings of two transmission spectra taken with and without a dc electric field, $\vec{E}_D$, applied across the diamond plate.[7] For convenience, we call this the dc technique. The light beam was first mechanically chopped and then focused on the sample. The transmitted signal was analyzed,

TABLE III. Numerical values of the physical constants of diamond as used in the present analysis.

η	Index of refraction	2.42
m	Mass of carbon atom	1.995×10^{-23} g
ρ	Mass density	3.4 g/cm^3
N	No. of unit cells per unit volume	8.87×10^{22}/cm^3
ω_j	Frequency of the $\vec{q}\approx 0$ optical phonon	1332 cm^{-1}
ω_0	He-Ne laser excitation frequency	15 800 cm^{-1}

synchronously detected, and recorded. A typical recording with $\vec{E}_D = 0$ and $\vec{E}_D \neq 0$, extended in the neighborhood of ω_j, is shown in Fig. 2 with the observed relative change $\Delta S/S$ being equal to $\Delta T/T$. Thus, from Eqs. (7c), (12), (13), (14), and (17) and the experimental values for $\Delta T/T$ and the applied field, we can estimate the absolute value of the Raman tensor component a.

Although simple in principle, the dc technique in general is neither convenient nor sensitive enough to allow a detailed study of the absorption band. In addition, the band is superimposed on the zero-field spectrum, which may be complicated because of the presence of structure of other origin, principally atmospheric absorption. Instead, a differential or ac technique can be used to discriminate against any signal not related to the field-induced band with subsequent increase of the sensitivity. In this method, an ac electric field (amplitude E_A) is applied on the crystal with the chopper removed from the beam. This induces an ac change ΔI in the transmitted intensity which is then amplified and recorded. The recorded band represents a signal proportional to ΔI versus the wavelength.

In recent years, several sophisticated techniques have been employed for the direct measurement of the ratio $\Delta T/T$ using two lock-in amplifiers and one recording for experiments involving relative changes of the transmittance.[22-24] This is necessary if the spectrum is rather extended and changes in ΔI not due to ΔT (such as wavelength variation of I_0) must be compensated by proportional changes in I, so that the ratio $\Delta I/I = \Delta T/T$ remains unchanged. In the present work, we were interested in a single band, only a few cm^{-1} broad, over which I_0 was practically constant. Therefore, we based our measurements on the observed field-induced signal ΔS, which gives all the necessary information for the characteristics of the band. A separate measurement, however, was made for the ratio $\Delta S/S = \Delta T/T$ which was required for the numerical determination of ΔA according to Eq. (17).

As already discussed the strength of the band is proportional to $|\vec{e}_{jE}|^2$, i.e., quadratic with the applied field $\vec{E}_a$. If we use a conversion parameter B, we can write for the signal seen by the detector in the ac technique that

$$\Delta I = I(0) - I(E_a) \equiv BE_a^2 \ , \tag{18}$$

where B is taken as independent of $\vec{E}_a$. Actually, by $\vec{E}_a$ we do not necessarily mean a pure dc or ac field applied on the one electrode and with the other one connected to the ground. In fact, we can replace the ground by a "bias" voltage (field) $V_D(E_D)$ to an arbitrary level, to be determined later. This gives rise to the bias-ac technique, whose advantage will be demonstrated later. The rest of this analysis refers to this technique.

The net applied field seen by the crystal, has the form

$$E_a = E_D - E_A \cos 2\pi ft \ , \tag{19}$$

where f is the modulation frequency. If Eq. (19) is inserted into Eq. (18), we find that

$$(\Delta I)_A = B(E_D^2 + \tfrac{1}{2}E_A^2) - 2BE_DE_A \cos 2\pi ft + \tfrac{1}{2}BE_A^2 \cos 4\pi ft \ , \tag{20}$$

where $(\Delta I)_A$ stands for the net field-induced signal that the detector passes to the lock-in amplifier. The first term simply designates a small dc reduction of the incident intensity, and is not passed through the lock-in amplifier. The second and third term can be detected separately, with the lock-in amplifier tuned to f and $2f$, respectively. One advantage of the bias-ac technique is now obvious. To obtain an adequate signal at $2f$ without bias, one needs a rather large E_A. With an appropriate bias field E_D, however, the same signal can be obtained at f using smaller values of E_A, a

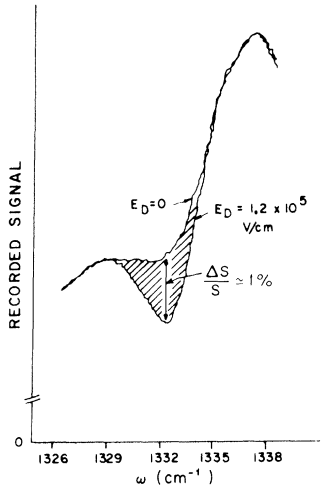

FIG. 2. Recorded transmission signal with zero and nonzero field. The relative change of the transmittance is about 1% for $E_D = 1.2\times10^5$ V/cm (sample C1).

procedure which is technically easier. In Fig. 3 the two terms are shown as recorded under identical conditions. The recorded peak signal can be written as

$$(\Delta S)_A = \beta(\Delta I)_A = -2\beta B E_D E_A \quad \text{detected at } f$$
$$= +\tfrac{1}{2}\beta B E_A^2 \quad \text{detected at } 2f, \qquad (21)$$

where β is a conversion parameter. As expected, the ratio of the two signals at the peak frequency (1332 cm^{-1}) of Fig. 3 is the same as the ratio $2BE_DE_A/\frac{1}{2}BE_A^2$ for the fields which were applied. Another important advantage of the bias-ac technique will be discussed later in Sec. V, namely, the combination of a modulation E_A and a bias E_D may reveal field-dependent terms of the R tensor $\overleftrightarrow{a}_{F_{2g}}$.

To determine the ratio $\Delta I/I$ at the single frequency of 1332 cm^{-1}, a separate measurement for I was taken, using the mechanical chopper and otherwise identical optical and electronic conditions. To ensure that the intensity conditions which are involved in the dc and bias-ac technique are the same, one should be careful in interpreting the signals I and ΔI. More explicitly, when the beam is chopped to yield a nearly symmetric square pulse, the transmitted light pulse has the following form:

$$I(0, t) = I\left(\frac{1}{2} + \frac{2}{\pi}\cos 2\pi f t - \cdots\right), \qquad (22a)$$

when no field is applied, and

$$I(E_D, t) = (I - BE_D^2)\left(\frac{1}{2} + \frac{2}{\pi}\cos 2\pi f t \cdots\right), \qquad (22b)$$

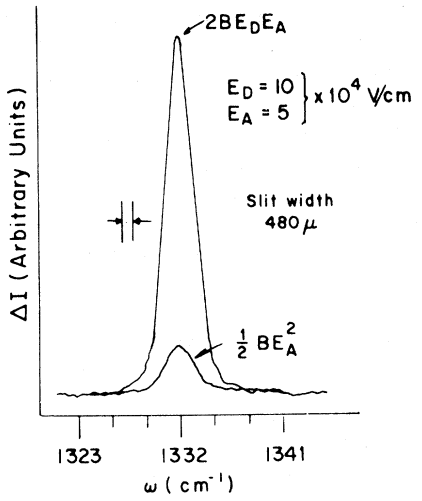

FIG. 3. Recorded transmission signal when a sinusoidal electric field of frequency f, together with a bias-dc field, is applied. The recordings at f and $2f$ are taken under otherwise identical conditions (sample $C2$).

when a dc field is applied. Since the lock-in amplifier is tuned to the chopping frequency f, only the fundamental term will be responsible for the observed relative change of the two recordings in Fig. 2, namely,

$$\Delta S = \beta I(0, f) - \beta I(E_D, f) = \beta(2/\pi)\, BE_D^2\,, \qquad (23)$$

where β is the same conversion factor, introduced earlier. This can be related to the recorded signal $(\Delta S)_A$ at f, when the bias-ac technique is applied, by using Eq. (21):

$$\Delta S = (V_D/\pi V_A)\,(\Delta S)_A\,. \qquad (24)$$

The ratio $\Delta T/T$ entering (22) now becomes

$$\Delta T/T = \Delta S/S = (V_D/\pi V_A)\,[(\Delta S)_A/S]\,, \qquad (25)$$

where $(\Delta S)_A$ is the recorded peak signal at 1332 cm^{-1} with the bias-ac technique employed, and S is just the recorded signal at 1332 cm^{-1} with the chopper on, and no field applied. Both $(\Delta S)_A$ and S are taken at the fundamental frequency of the modulation and the chopper, respectively.

The connection between theory and experimental parameters can now be established, through Eqs. (7c), (12)–(14), (17), and (25). For the three configurations of Table I, one finds the following expressions for the R tensor in terms of $(\Delta S)_A/S$:

$$a^2 = \frac{\bar{m}\eta c}{4.24\pi^2 N}\,\frac{\xi\gamma d^2}{V_D V_A l}\,\frac{(\Delta S)_A}{S}\,, \qquad (26)$$

where d is the thickness of the sample. ξ has the values 1, 3, $\frac{3}{4}$ for the configurations $C1$, $\hat{\epsilon}_0 \perp \hat{\epsilon}_a$; $C2$, $\hat{\epsilon}_0 \perp \hat{\epsilon}_a$; and $C2$, $\hat{\epsilon}_0 \parallel \hat{\epsilon}_a$; respectively, and γ is determined from the half-width of the observed band. Equation (26) gives the absolute value of the R tensor a for diamond, in terms of physical and experimental parameters.

B. Apparatus

In Fig. 4 the block diagram of the experimental setup is shown. A "4-mm Nernst glower" IR light source was used, operating at a current of 0.8–1.0 A. The IR polarizer was a Perkin-Elmer stack of AgCl plates. A Perkin-Elmer (model 12C) grating monochromator was used to analyze the light. The grating was a Bausch and Lomb with 150 lines/mm, while a band pass interference filter (6.5-10.5μ) was used to cut off second and higher orders. A Reeder thermocouple detector was initially used with a 13 cps reciprocating chopper. Later, it was replaced by a gold-doped Ge detector operating at liquid nitrogen temperature and sensitive in the region between 2 and 9 μ. In this case, a PAR (type BZ-1) chopper was used at 600 cps. The over-all sensitivity was significantly improved. A PAR lock-in amplifier (type HR-8) was also used with type B or A preamplifier,

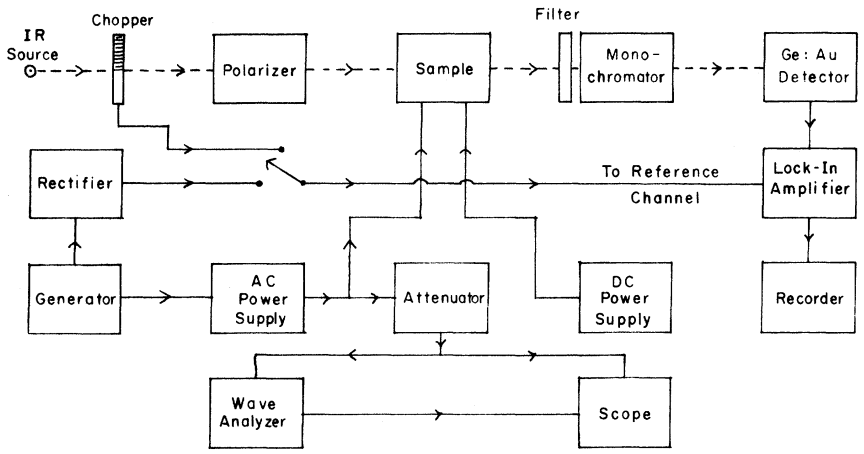

FIG. 4. Block diagram of the experimental set-up.

when the thermocouple or Ge:Au detector was employed, respectively. The high-voltage sinusoidal modulator was especially designed to give up to 15 kV peak to peak, with a maximum of 70 V peak to peak in the input supplied by a standard oscillator. The distortion of the waveform was less than 0.2% for the second and third harmonic, as measured by a GR (type 1900/A) wave analyzer through a 1000:1 attenuator.[25] The reference for the lock-in was taken either from the chopper, or from the oscillator through a half- or full-wave rectifier, to enable us to use the lock-in at any of the frequencies desired, i.e., f, $2f$, $3f$.

The two type-IIa polished and oriented diamond samples were kindly provided by the Diamond Research Laboratory, Johannesburg, South Africa.

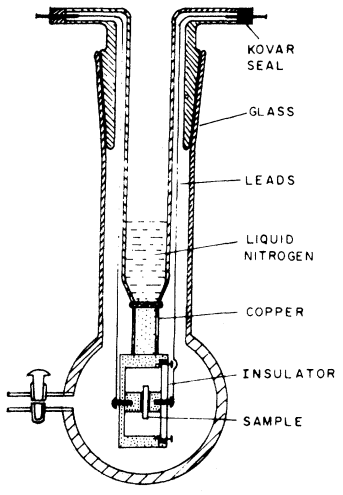

FIG. 5. Home-made glass cell for the transmission measurements at 80 °K in the presence of an electric field. The light is directed perpendicularly to the plane of the figure.

The sample cell, made of glass with KBr windows, is shown in detail in Fig. 5. To apply sufficiently high fields, it was necessary to keep the system in vacuum ($\sim 10^{-6}$ Torr) at liquid nitrogen temperature. For the same reason we avoided evaporated silver or gold films as electrodes, which were easily carbonized every time an accidental arcing occurred around the diamond plate. Instead, the plate was gently held between two copper blocks which were highly polished to assure good contacts. The area of contact was slightly smaller than the face of the sample, and this reduced the arcing significantly. Accordingly, a correction was made in considering the effective light path l, through the plate (Table I). No measureable current was observed through the crystal even at the highest applied dc field (2×10^5 V/cm). The applied dc voltage was measured within 2%, with the meter of the voltage supply ("Universal Voltronics"). The ac voltage was measured either with an oscilloscope, or with a wave analyzer within the same accuracy.

Although the field appearing in the previous analysis is strictly the macroscopic field in the crystal, we assume that this is given by V/d, i.e., that there is no depolarizing field. This can be achieved, either by choosing the crystal to be a thin slab parallel to the field, or by plating the electrodes on the faces of the crystal. It turned out that the technique described above was effectively the same.

IV. RESULTS

According to Eq. (21), the strength of the band $(\Delta S)_A$ is linear with E_D or E_A if detected at f, and quadratic with E_A only, if detected at $2f$. To test this, the spectrometer was fixed at the wavelength of the maximum signal $(\Delta S)_A$, with a slit width of 480 μ which was wide enough for a sufficient signal. A time constant of 100 sec was necessary to keep

the noise level down. Figures 6, 7, and 8 show the results which are in excellent agreement with Eq. (21).

To study the width of the band, the slit was closed down to 160 μ in order to reduce the instrumental broadening. At this slit width the instrument resolution was 0.5 cm^{-1}. Again, a long time constant was necessary. To be sure that the time constant did not affect the position and the width of the band, a point-by-point run was taken as shown in Fig. 9 for the $C1$, $\hat{\epsilon}_0 \perp \hat{\epsilon}_a$ configuration. To the band width indicated, an estimated correction of 0.5 cm^{-1} was subtracted, to account for the instrumental broadening. The numerical results at room and liquid nitrogen temperature are presented in Tables IV and V. The spectrometer was calibrated against CH_4 gas lines, within 0.05 cm^{-1}, and the signal-to-noise ratio was at least as good as 50:1.

The ratio $(\Delta S)_A/S$ was found to be strongly dependent on the slit width. We, therefore, had to measure and plot $(\Delta S)_A/S$ for several slit widths, and then extrapolate to zero width, to obtain the real ratio at liquid nitrogen temperature. The extrapolation seems to be the main source of error in calculating the absolute value of the R tensor, in spite of considerable experimental effort to minimize it. The results are shown in Fig. 10.

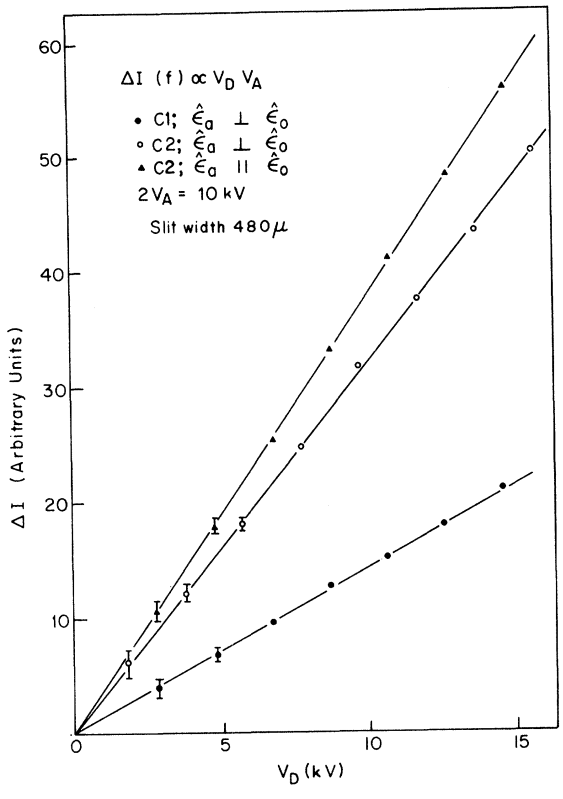

FIG. 6. Observed peak-intensity at 1332 cm^{-1} versus V_D, keeping V_A constant. The bias-ac technique is used with the fundamental component of the signal detected at the modulation frequency f.

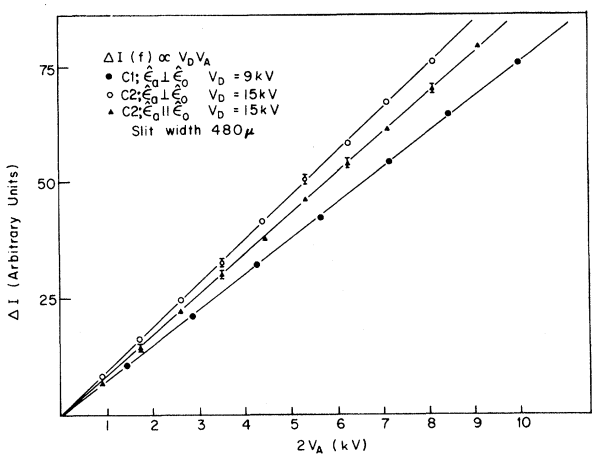

FIG. 7. Observed peak-intensity at 1332 cm^{-1} versus V_A, keeping V_D constant. The bias-ac technique is used with the fundamental component of the signal detected at the modulation frequency f.

Even at the highest available applied fields (2×10^5 V/cm) and with conditions of maximum signal we were unable to observe any shift or splitting of the triply degenerate mode.[26] This is consistent with the result of Ref. 14, where it is predicted that for these fields, shifts and splittings should be expected of the order of magnitude of 10^{-4} cm^{-1}. This is far below the usual experimental

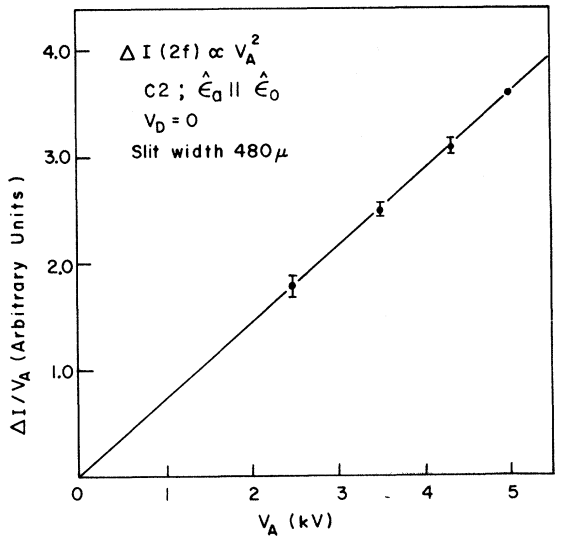

FIG. 8. Observed peak-intensity at 1332 cm^{-1} versus V_A^2, with $V_D = 0$. The plain ac technique is used with the second harmonic of the signal detected at $2f$.

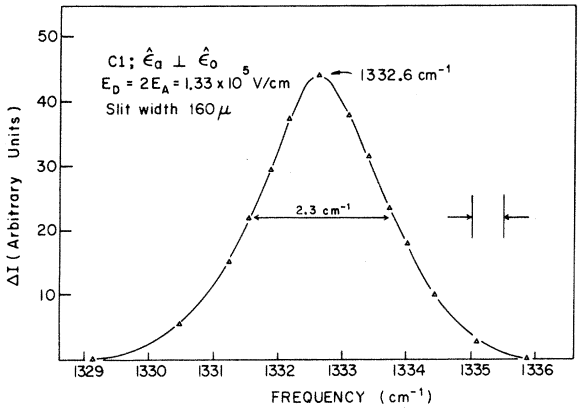

FIG. 9. Point-by-point run of the field-induced band, with a minimum slit width, corresponding to an instrumental broadening of about 0.5 cm^{-1} (configuration $C1$, $\hat{\epsilon}_0 \perp \hat{\epsilon}_a$).

limits set by the instrumental resolution. Also, we were not able to observe any meaningful change in the linewidth with different fields. Since the change is expected to be quadratic in the electric field (it is a higher-order effect), we feel that such changes might be observable only with interferometric techniques, in connection with a Raman scattering experiment.

Finally, the first-order Raman efficiency per unit crystal length per unit solid angle with unpolarized incident and scattered light is found to be 3×10^{-7}. (Loudon's rough estimate based on deformation potential arguments places it between 10^{-6} and 10^{-7}.[3]) The equation

$$S = 3\hbar\omega_S^4 N^2 a^2/\rho c^4 \omega_j (n_0+1) \qquad (27)$$

TABLE V. Other numerical results.[a]

$\lvert\Delta A\rvert$ [b] cm^{-1}	$\lvert e_{F_{2g}E}/e\rvert$ [c]	S_C^d	S_{Si} [e]	S_{Ge} [f]
$1.5\times10^{-6}E_D^2$	$0.8\times10^{-6}E_D$	3.0×10^{-7}	1.0×10^{-5}	1.0×10^{-6}

[a]The values of 4×10^{-16} cm^2 and 1 cm^{-1} have been taken for $\lvert a\rvert$ and γ, respectively; the field E_D is in cgs units.
[b]From Eq. (12).
[c]$e_{F_{2g}E}$ corresponds to Eq. (7c).
[d]From Eq. 27.
[e]From Ref. 20 and present results.
[f]From Refs. 20 and 21 and present results.

was used,[19,27] where $\omega_S = \omega_0 - \omega_j$, ρ is the crystal density and $n_0+1 \simeq 1$ at 300 °K and 77 °K, for diamond.

V. FIELD DEPENDENCE OF RAMAN TENSOR

In writing the relation between the transmitted intensity changes and the applied field, i.e., Eq. (18), we made the assumption that B was independent of the applied field. This is equivalent to assuming the R tensor $\overleftrightarrow{a}$ to be independent of the field, or assuming the field-induced effective charge to be simply linear with the field. To a higher approximation, one can write the equation for $\vec{e}_{jE}$, after suppressing the index $j = F_{2g}$, as

$$e_{jE} = (a + A^{(2)}E_a^2)E_a \ , \qquad (28)$$

where $2A^{(2)} = d^2a/dE_a^2$ is the second total derivative of $\overleftrightarrow{a}_{F_{2g}}$ with respect to the applied field, rather than the partial derivative. It includes contributions to the change of $\overleftrightarrow{a}_{F_{2g}}$ from electrostriction and field-induced lattice displacements, both quadratic with the field.[28] The first-order terms (da/dE_a) do not exist in diamond-type crystals. A further discussion of the nature and symmetry of the co-

TABLE IV. Summary of the present results and comparison with those of other workers.

Configuration[a]	ω_j [b] (cm^{-1})		Width[b] 2γ(cm^{-1})		$\lvert a\rvert$	$A^{(2)}/a$ cgs	$\lvert a_{Si}\rvert$	$\lvert a_{Ge}\rvert$
	300 °K	77 °K	300°K	77 °K	Å^2		Å^2	Å^2
$C1$; $\hat{\epsilon}_0 \perp \hat{\epsilon}_a$	1332.10 1331.80[e] 1332.50[g]	1332.60 1333.20[e] 1333.30[g]	2.00 3.40[e]	1.80	3.40 4.00[f]	-1×10^{-8}	10.80[c]	21.6 – 13.5[c,d]
$C2$; $\hat{\epsilon}_0 \perp \hat{\epsilon}_a$	1331.90	1332.60	1.80	1.60	4.40 4.60[f]		7.0[h]	12.0[h]
$C2$; $\hat{\epsilon}_0 \parallel \hat{\epsilon}_a$	1331.95	1332.55	1.75	1.50	3.50 3.80[h]			

[a]Results e, h, i do not necessarily correspond to the configuration indicated.
[b]Present results within ±0.05 cm^{-1}.
[c]Reference 20.
[d]Reference 21.
[e]Reference 33.
[f]Reference 7.
[g]According to recent measurements by S. A. Solin and A. K. Ramdas, Phys. Rev. B 1, 1687 (1970).
[h]Reference 32.
[i]Reference 34.

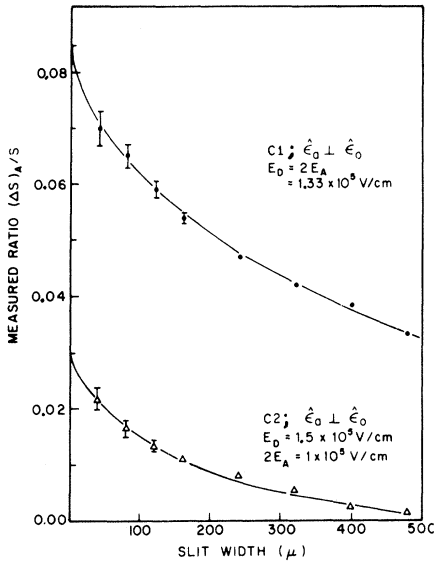

FIG. 10. The observed ratio $(\Delta S)_A/S$ versus slit width for two of the configurations. The third configuration $C2$, $\hat{\epsilon}_0 \parallel \hat{\epsilon}_a$ almost coincides with the $C1$, $\hat{\epsilon}_0 \perp \hat{\epsilon}_a$ with an extrapolated value at 0.08 for the ratio $(\Delta S)_A/S$.

efficient $A^{(2)}_{F_{2g}}$ can be found in Ref. 28.

In what follows we will try to describe how, with a simple experimental arrangement, it is possible to identify and eventually measure the second-order term of the R tensor.

It is clear, from Eqs. (12), (13) and (17) that the theoretical ratio $\Delta T/T$ of Eq. (17) can be written as

$$\Delta T/T = De^2_{jE} ,$$

where

$$D \equiv -4.24\pi Nl/\bar{m}\gamma c\eta_1 .$$

On the other hand, Eq. (28) gives

$$e^2_{jE} = a^2E^2_a + 2aA^{(2)}E^4_a + (A^{(2)}E^3_a)^2 \simeq a^2E^2_a + 2aA^{(2)}E^4_a ,$$

and therefore,

$$\Delta T/T = DE^2_a[a^2 + 2aA^{(2)}E^2_a] . \quad (29)$$

From experimental point of view, we can write down an expression similar to Eq. (23), i.e.,

$$\Delta S = \beta(2E^2_D/\pi)(B + CE^2_D) . \quad (30)$$

From (29) and (30) with $\vec{E}_D = \vec{E}_a$, we find by comparison that

$$C/B = 2A^{(2)}/a; \quad (31)$$

i.e., any experimental information about the ratio C/B would immediately make possible an estimation of $A^{(2)}$.

If the bias-ac technique is to be used, Eq. (18) becomes

$$(\Delta I)_A = BE^2_a + CE^4_a .$$

With $E_a = E_D - E_A\cos\theta$, $\theta = 2\pi ft$ and after some algebra, one finds that

$$(\Delta I)_A = \lambda_0 + \lambda_1\cos\theta + \lambda_2\cos 2\theta + \lambda_3\cos 3\theta + \lambda_4\cos 4\theta, \quad (32)$$

where

$$\lambda_0 = B(E^2_D + \tfrac{1}{2}E^2_A) + 3CE^2_A(E^2_D + \tfrac{1}{8}E^2_A) , \quad (33a)$$

$$\lambda_1 = -2BE_DE_A - 4CE^3_DE_A - 3CE_DE^3_A , \quad (33b)$$

$$\lambda_2 = \tfrac{1}{2}BE^2_A + 3CE^2_DE^2_A + \tfrac{1}{2}CE^4_A , \quad (33c)$$

$$\lambda_3 = -CE_DE^3_A , \quad \lambda_4 = \tfrac{1}{8}CE^4_A . \quad (33d)$$

It is clear that if we set $C = 0$, Eqs. (32) and (33) are reduced to Eq. (20). It also follows from Eq. (32) that, as the lock-in amplifier is tuned at the frequencies f, $2f$, $3f$, $4f$, the observed signal is proportional to λ_1, λ_2, λ_3, λ_4, respectively.

In plotting λ_1 versus E_D (Fig. 6) we were unable to observe any nonlinearity well above the noise level. We therefore turned our attention to the second-harmonic term λ_2. If we ignore the last term of λ_2, the higher-order term $3CE^2_DE^2_A$ is expected to appear as a small change of the signal $\frac{1}{2}BE^2_A$, when E_D is turned from zero to a nonzero and rather high value. The observed fractional change

$$3CE^2_DE^2_A/\tfrac{1}{2}BE^2_A = 6E^2_D(C/B)$$

can then provide a numerical value for the ratio $A^{(2)}/a$, according to Eq. (31). In principle, any signal detected at $3f$ and $4f$ would be exclusively due to C. However, these terms are expected to be rather small judging from their ratio to the leading term of (33c). Any distortion of the voltage modulation in the form of second and third harmonic would also introduce a signal due to the major term $2BE_DE_A(2f, 3f)$, when the amplifier is tuned at $2f$ or $3f$, respectively. We therefore made sure that the distortion level was less than 0.2%, which makes the above spurious signal negligible.

With the lock-in amplifier tuned at $2f$, and a suitable reference taken from the oscillator through a rectifier (Fig. 4) we observed a negative change of about 10% with $V_D = 12$ kV, $V_A = 5$ kV in the $C1$, $\hat{\epsilon}_0 \perp \hat{\epsilon}_a$ configuration. Since the signal-to-noise ratio was not better than 4:1, we can only say that the ratio $A^{(2)}/a$ is of the order of -1×10^{-8} cgs.

The observability of this nonlinearity in the IR suggested the possibility of observing an electric-field-modified R scattering in diamond due to $A^{(2)}$-type changes of the R tensor in the presence of the field. Further, we note that $A^{(2)}$, defined in Eq. (28), is expected to have a definite symmetry and matrix form, consistent with the symmetry of the

diamond structure. It will be shown later that the measured component in this specific configuration was $A^{(2)}_{23133} = \frac{1}{2}(d^2 a_{231}/dE_3 dE_3)$, as referred to the xyz axes. In Sec. VI we discuss the role of the nonlinear term $A^{(2)}$ in R scattering.

VI. EFFECT OF AN APPLIED ELECTRIC FIELD ON RAMAN SCATTERING IN DIAMOND

A. Symmetry Arguments

As already pointed out in the previous section, the R tensor $\overleftrightarrow{a}_{F_{2g}}$ exhibits a quadratic dependence on the applied field, which would manifest itself as a change in the intensity of R scattering and/or a modification of the polarization selection rules. A complete discussion on the symmetry considerations in connection with R scattering in the presence of external forces can be found in Ref. 2. In particular, the matrix form of the strain-induced R tensor $\overleftrightarrow{a}_{F_{2g}\eta}$ of diamond is identical with the matrix form for the field-induced R tensor in second order in the field $\overleftrightarrow{a}_{F_{2g}EE}$, (a homogeneous strain η_{lm} and a field in second $E_l E_m$ are "forces" with the same symmetry). When transcribed for an electric field, the matrix form of $\overleftrightarrow{a}_{F_{2g}\eta}$ derived in Ref. 2 is given by

$$\overleftrightarrow{a}_{F_{2g}EE} = \begin{bmatrix} cE_2E_3 & fE_3E_1 & fE_1E_2 \\ fE_3E_1 & eE_2E_3 & bE_1^2 + d(E_2^2 + E_3^2) \\ fE_1E_2 & bE_1^2 + d(E_2^2 + E_3^2) & eE_2E_3 \end{bmatrix},$$

$$\begin{bmatrix} eE_3E_1 & fE_2E_2 & bE_2^2 + d(E_3^2 + E_1^2) \\ fE_2E_3 & cE_3E_1 & fE_1E_2 \\ bE_2^2 + d(E_3^2 + E_1^2) & fE_1E_2 & eE_3E_1 \end{bmatrix},$$

$$\begin{bmatrix} eE_1E_2 & bE_3^2 + d(E_1^2 + E_2^2) & fE_2E_3 \\ bE_3^2 + d(E_1^2 + E_2^2) & eE_1E_2 & fE_3E_1 \\ fE_2E_3 & fE_3E_1 & cE_1E_2 \end{bmatrix},$$

for the phonon components which transform like (yz), (zx), and (xy), respectively. The parameters $2b$, $2c$, $2d$, $2e$, f are the five independent components[2] of the coefficient $(d^3\alpha/du_{F_{2g}} dE dE)$; the indices are referred to the xyz system and the electronic polarizability is again treated as a second-rank symmetric tensor.

In the presence of an electric field, the total R tensor for diamond is given by,

$$\overleftrightarrow{a}(F_{2g}, \vec{E}\vec{E}) \simeq \overleftrightarrow{a}_{F_{2g}} + \overleftrightarrow{a}_{F_{2g}EE}, \tag{34a}$$

where

$$\overleftrightarrow{a}_{F_{2g}EE} = \tfrac{1}{2}(d^3\overleftrightarrow{\alpha}/du_{F_{2g}} dE dE) \cdot \vec{E}\vec{E}. \tag{34b}$$

The diamond sample $C1$ which was used allowed application of an electric field only along the [001] direction, i.e., $E_1 = E_2 = 0 \neq E_3$. From the matrix forms for $\overleftrightarrow{a}_{F_{2g}}$, $\overleftrightarrow{a}_{F_{2g}EE}$ and (34a) one finds for $\overleftrightarrow{a}(F_{2g}, \vec{E}\vec{E})$

$$u_{F_{2g}}: \quad \begin{bmatrix} 0 & 0 & 0 \\ 0 & 0 & a + dE_3^2 \\ 0 & a + dE_3^2 & 0 \end{bmatrix} (yz), \quad \begin{bmatrix} 0 & 0 & a + dE_3^2 \\ 0 & 0 & 0 \\ a + dE_3^2 & 0 & 0 \end{bmatrix} (zx), \quad \begin{bmatrix} 0 & a + bE_3^2 & 0 \\ a + bE_3^2 & 0 & 0 \\ 0 & 0 & 0 \end{bmatrix} (xy), \tag{35}$$

i.e., for this direction of the field one should see only a change of the strength of the field-free R scattering. The polarization selection rules do not change, since the induced R tensor components appear in the same places as the field-free Eq. (4b). Should the field be applied in a direction other than [001], the situation would be different. In the (6×3) matrix notation the matrices of Eq. (35) can be written as

$$\overleftrightarrow{a}(F_{2g}, \vec{E}\vec{E}) = \begin{bmatrix} 0 & 0 & 0 \\ 0 & 0 & 0 \\ 0 & 0 & 0 \\ a + dE_3^2 & 0 & 0 \\ 0 & a + dE_3^2 & 0 \\ 0 & 0 & a + bE_3^2 \end{bmatrix}, \quad \begin{bmatrix} 0 & 0 & -(a + bE_3^2) \\ 0 & 0 & a + bE_3^2 \\ 0 & 0 & 0 \\ 0 & a + dE_3^2 & 0 \\ -(a + dE_3^2) & 0 & 0 \\ 0 & 0 & 0 \end{bmatrix}, \tag{36}$$

when expressed in the two systems of axes xyz and $x'y'z'$, respectively. (The geometry of the sample C1 as described in Table I is followed.) It is noted that a is the only single independent component of $\overleftrightarrow{a}_{F_{2g}}$ and b, d are given by

$$2b=\left(\frac{d^3\alpha_{12}}{du_3 dE_3 dE_3}\right),\quad 2d=\left(\frac{d^3\alpha_{13}}{du_2 dE_3 dE_3}\right)=\left(\frac{d^3\alpha_{23}}{du_1 dE_3 dE_3}\right), \tag{37}$$

with the indices referred to the xyz axes in accordance with Eqs. (34), and (35).

For an experiment performed with $C1$ in the $-x'(y'z')x'$ configuration,[29] the observed intensity of the R line is proportional to a^2 and $(a+dE_3^2)^2$ for $E_3=0$ and $E_3\neq 0$, respectively, according to Eq. (36). Thus, the observed change in the R intensity, when a field is applied, is proportional to

$$(a+dE_3^2)^2-a^2=2adE_3^2+d^2E_3^4\simeq 2adE_3^2 \tag{38}$$

for $dE_3^2\ll a$. Therefore, from the observed fractional change $2adE_3^2/a^2$, one can deduce a numerical value for the coefficient d. In a similar manner, a value for b can be obtained from the ratio $2abE_3^2/a^2$ which can be observed in an experiment performed in the $-x'(y'y')x'$ configuration.

B. Experimental Results

Measurements were made using the University of Pennsylvania Raman spectrometer designed and built by Filler, and a He-Ne laser excitation frequency at 15 800 cm^{-1}. The optical layout and block diagram are shown in Fig. 11. The diamond plate shown in Fig. 1 was kept in the glass vacuum cell, at 80 °K. In scanning through the Stokes-Raman line, two measurements were made at each grating position, one with field and one without field. The transistorized dc voltage supply was turned on and off electronically through a relay for equal time intervals. A typical run is

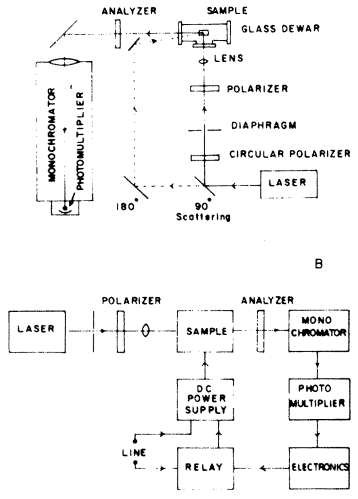

FIG. 11. Optical layout (a) and block diagram (b) of the R scattering experiments with an applied electric field.

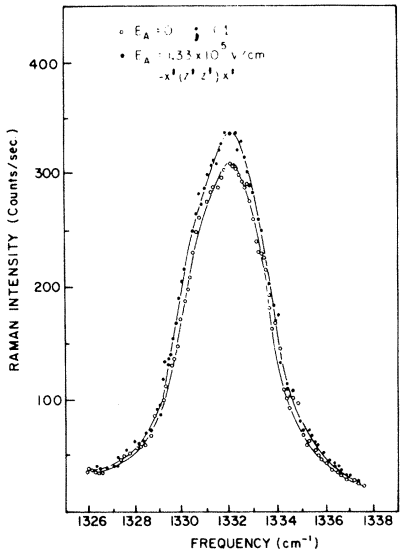

FIG. 12. Typical run (with and without an electric field) of the first order R line of diamond in the $-x'(z'z')x'$ geometry and $C1$ sample. Instrumental resolution $\simeq 2$ cm^{-1}.

shown in Fig. 12 for a field of 1.33×10^5 V/cm. A circular polarizer was placed before the linear polarizer in the incident beam, to assure equal incident intensity for any polarization.

With the field parallel to the z' axis, the symmetry analysis presented in the previous section applies. Back-scattering measurements were carried out on the type-IIa $C1$ diamond plate, first in the configuration $-x'(z'z')x'$, which according to the matrix form [Eq. (36)] should lead to no R scattering, regardless of an applied field. Instead, a weak peak was observed which was initially attributed to misalignment and residual strain birefringence. Careful alignment, however, did not improve the situation (furthermore, examination between crossed polarizers indicated strong residual strain birefringence.[30,31] When an electric field was applied in the $-x'(z'z')x'$ configuration, an increase in the intensity was observed, which was quadratic with the field (Fig. 13) in agreement with Eq. (38). Because of the residual birefringence, it is reasonable to expect a mixing of the configurations $-x'(y'y')x'$ and $-x'(y'z')x'$ or $-x'(z'y')x'$ even when the experimental geometry has been set up for the configuration $-x'(z'z')x'$. Thus, the observed quadratic change can be attributed to the presence of terms of d and b character. Of course nothing can be said about their numerical values, since the way they mix is not known. Partially responsible for this mixing can also be the finite convergence of the scattered beam.

Measurements in the $-x'(y'z')x'$ configuration gave an approximate value of -1×10^{-8} cgs for the

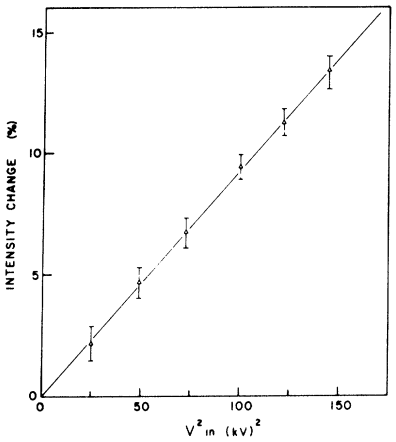

FIG. 13. Electric field dependence of the intensity change of the first-order R line shown in Fig. 12.

ratio d/a which agrees with the value obtained from the experiment in the IR (Sec. V). The absolute value of a can be taken from Table IV, while it sign has been established theoretically as (+).[32] No meaningful data were possible in the configuration $-x'(y'y')x'$, because of a poor signal-to-noise ratio. From the obtained estimate of d, we conclude that, for a configuration which would allow this coefficient to occur alone, it would lead to a field-induced intensity proportional to $(dE^2)^2$ which for the available fields is far below the noise level and would therefore be undetectable. In other words, the mixing $2adE^2$ of the linear and nonlinear components of the R tensor acts as a "bias" to amplify the effect of the field.

The present observation introduces in R spectroscopy a procedure for detecting a small coefficient through its product with a larger known parameter. By rotating either the crystal or the polarizers through a small angle, one can introduce an arbitrary amount of "bias" and thereby obtain a numerical value for the small coefficient.

VII. SUMMARY

In this article, the first-order resonance absorption of the EM radiation by optical vibrational modes is examined in connection with an applied electric field. Our experimental results on the field-induced IR absorption in type-IIa diamond are presented, together with the necessary analysis which leads to the main task of this work, namely, the experimental determination of the R tensor component for diamond. In Tables IV and V summary of our results is presented, together with other workers' results, wherever they are available.

In view of our improved experimental resolution, we feel that our values of the diamond's half-width are more accurate than those obtained elsewhere through direct R scattering measurements.[33]

The value for the R tensor $|a| = 4\times10^{-16}$ cm^2, previously reported,[7] is again confirmed. Meanwhile, other workers have reported similar values. McQuillan and co-workers[34] have recently obtained the value of 4.6×10^{-16} cm^2 from independent measurements of the R scattering efficiency in diamond. It should be noted in this connection that the field-induced absorption and R scattering efficiency data can only provide information about the absolute magnitude of a. Maradudin and Burstein[32] have recently derived the sign and magnitude of a for diamond-type crystals from experimental values of the photoelastic constants using a microscopic lattice theory which relates the photoelastic and R tensors. They obtain $a = +3.8\times10^{-16}$ cm^2 for diamond,[35] $a = -7\times10^{-16}$ cm^2 for silicon, and $a = +12\times10^{-16}$ cm^2 for germanium. The results for silicon and germanium are rather uncertain largely because of the large uncertainty in the photoelastic data.

No effect of the field on the linewidth was observed, nor did any shift or splitting of the triply degenerate mode become evident, in agreement with theoretical predictions. We did, however, observe a field-dependent term in the R tensor which was further confirmed by independent R scattering experiments in the presence of a field. It turns out that crystal imperfections interfere critically with the precision of R experiments of this type. R scattering measurements yielded a value for the associated nonlinear coefficient of diamond, which is in agreement with the results obtained by the IR absorption experiments.

ACKNOWLEDGMENTS

We acknowledge with appreciation the help of A. Filler in the spectroscopic and electronic aspects of the present work. We are indebted to Dr. L. BuPreez and S. M. Horszowski of the Diamond Research Laboratory, Johannesburg, South Africa, for the supply of diamond samples, and Dr. D. E. Bode of the Santa Barbara Research Center for providing the Ge : Au samples for the IR detector. Valuable discussions with M. Whippman, A. Pinzuck, C. Bucci, and W. Taylor are also acknowledged. Finally, the experimental contribution of S. Iwasa in the early stage of this work is greatly appreciated.

Note added in proof. One of us (E. A.) thanks Sir C. V. Raman for bringing to his attention his latest findings on diamond.

*Work supported by the U. S. Office of Naval Research.

†Present address: Physics Department, Northeastern University, Boston, Mass. 02115.

‡Work based in part on Ph. D. thesis submitted at the University of Pennsylvania, 1968.

[1]M. Lax E. Burstein, Phys. Rev. 91, 39 (1955).

[2]E. Anastassakis and E. Burstein, J. Phys. Chem. Solids (to be published).

[3]R. Loudon, Proc. Roy. Soc. London A275, 218 (1963).

[4]H. Mueller, Phys. Rev. 47, 947 (1935).

[5]E. Burstein and S. Ganesan, J. Phys. (Paris) 26, 637 (1965).

[6]B. Szigetti, Diamond Conference, 1965 (unpublished).

[7]E. Anastassakis, S. Iwasa, and E. Burstein, Phys. Rev. Letters 17, 1051 (1966); 18, 227(E) (1967).

[8]E. V. Condon, Phys. Rev. 41, 759 (1932).

[9]M. F. Crawford and I. R. Dagg, Phys. Rev. 91, 1569 (1953).

[10]M. F. Crawford and MacDonald, Can. J. Phys. 36, 1022 (1958).

[11]E. Burstein, A. Maradudin, E. Anastassakis, and A. Pinczuk, Helv. Phys. Acta 41, 730 (1968).

[12]A. A. Maradudin and R. F. Wallis, Phys. Rev. 123, 777 (1961).

[13]R. F. Wallis and A. A. Maradudin, in *Proceedings of the International Conference on the Physics of Semiconductors, Exeter, July*, 1962, edited by A. C. Stickland (The Institute of Physics and the Physical Society, London, 1962), p. 490.

[14]S. Ganesan, A. A. Maradudin, and J. Oitmaa, Ann. Phys. (N. Y.) 56, 556 (1970).

[15]H. Hartman, Phys. Rev. 47, 663 (1966).

[16]Since 2γ is the observed full width at half-intensity of the induced absorption band, a numerical value for γ can be obtained directly from the experiment.

[17]The dependence of ω_j on the applied field in second order is with symmetry the same as that on an applied homogeneous uniaxial stress. For the latter, see E. Anastassakis, A. Pinzuck, E. Burstein, F. Pollak, and M. Cardona, Solid State Commun. 8, 133 (1970).

[18]J. F. Nye, *Physical Properties of Crystals* (Oxford U. P., London, 1964).

[19]R. Loudon, Advan. Phys. 13, 423 (1964).

[20]J. P. Russell, Appl. Phys. Letters 6, 223 (1965).

[21]J. H. Parker, Jr., D. W. Feldman, and M. Ashkin, Phys. Rev. 155, 712 (1967).

[22]Y. Hamakawa, F. A. Germano, and P. Handler, Phys. Rev. 167, 703 (1968).

[23]R. Ludeke and P. William, Phys. Rev. 167, 736 (1968).

[24]C. Rhyner and J. R. Cameron, Phys. Rev. 169, 710 (1968).

[25]The circuit for the high voltage sinusoidal modulator was designed by A. Filler and later improved by M. Feldman of the University of Pennsylvania Physics Department. The authors are grateful to both of them for their help in this matter.

[26]In Ref. 7 a shift of 4 cm^{-1} was reported. It was later discovered that this was due to an instrumental error.

[27]H. Smith, Phil. Trans. Roy. Soc. London A241, 105 (1948).

[28]E. Anastassakis, A. Filler, and E. Burstein, in *Light Scattering in Solids*, edited by G. Wright (Springer-Verlag, New York, 1969).

[29]T. C. Damen, S. P. Porto, and B. Teller, Phys. Rev. 142, 570 (1966).

[30]A. R. Lang, Nature 213, 248 (1967).

[31]E. Anastassakis and E. Burstein, Solid State Commun. (to be published).

[32]A. A. Maradudin and E. Burstein, Phys. Rev. 164, 1081 (1968).

[33]R. S. Krishnan, Proc. Indian Acad. Sci. A 24, 45 (1946).

[34]A. K. McQuillan, W. R. L. Clements, and B. P. Stoicheff, Phys. Rev. A 1, 628 (1970).

[35]A (−) sign appears in Ref. 32. According to these authors, a calculational mistake was discovered and the sign should be changed to a (+).